No. 560 **February 2017**

Natural convection of gas along a vertical wavy surface with effect of variable thermophysical properties

A.A.A.A. Al-Rashed, S. Siddiqa, N. Begum, Md. A. Hossain

ISSN: 2190-1767

Natural convection of gas along a vertical wavy surface with effect of variable thermophysical properties

Abdullah A. A. A. Al-Rashed[†], Sadia Siddiqa[*,1], Naheed Begum[♭], Md. Anwar Hossain[‡]

[‡]*Department of Automotive and Marine Engineering Technology, College of Technological Studies, Kuwait city, Kuwait*

[*]*Department of Mathematics, COMSATS Institute of Information Technology, Kamra Road, Attock, Pakistan*

[♭]*Institute of Applied Mathematics (LSIII), TU Dortmund, Vogelpothsweg 87, D-44221 Dortmund, Germany*

[‡]*UGC Professor, Department of Mathematics, University of Dhaka, Dhaka, Bangladesh*

Abstract: The intent of this paper is to establish the detailed parametric study for laminar natural convection flow along a vertical wavy plate. Typical sinusoidal surface is used to elucidate the heat transport phenomena for the gas having variable thermophysical properties. From the present analysis, we will interrogate whether the presence of roughness element disturbs the gas flow and alter the physical characteristics associates with the wavy surface or not? The numerical solutions are obtained after converting the governing equations into a suitable coordinate system. The results are interpreted for the parameters which emerge from the temperature dependent physical properties of the gases and transverse curvature of the surface. In order to ensure the accuracy, the present numerical results are also compared with some special cases and are found in good agreement. The key observation from the present analysis is that the amplitude of wavy surface parameter, a contributes in reduction of heat transfer rate.

Keywords: Natural Convection, Variable Thermophysical Properties, Wavy Surface

1 Introduction

The analysis of the variable thermophysical properties of the fluid for laminar natural convection past an isothermal vertical wall has been reported by Sparrow and Gregg [1].

[1]Corresponding author.
Email: saadiasiddiqa@gmail.com

In this paper, the authors presented the solutions of the boundary layer equations for some special cases. After that, Brown [2] investigated the influence of the volumetric expansion coefficient on heat transfer rate for the problem of laminar free convection. In addition, Gray and Giogini [3] discussed the validity of the Boussinesq approximation for liquids and gases and proposed a method for analyzing natural convection flows with fluid properties. In this study, the authors assumed the physical properties of the fluid to be linear functions of temperature and pressure. It is important to mention here that, Clausing and Kempka [4] investigated the effect of variable properties on experimental basis and concluded that, for the laminar region, the rate of heat transfer Nu will be a function of Ra, only with reference temperature, T_f, which is taken as the average temperature in the boundary layer. Furthermore, the analysis of instability of laminar free convection flow and then the transition to turbulent state had been presented by Gebhart [5] and also have been summarized in a textbook by Eckert and Drake [6]. A detailed analysis of effect of variable thermophysical properties on laminar free convection of gas has also been presented in [8].

It is worthy to mention that all the above studies examined smooth surfaces only. Perhaps irregular surfaces are sometimes more important in industries, for instance, solar collectors, condensers in refrigerators, cavity wall insulating systems, grain storage containers, and industrial heat radiators are a few of the many applications of rough surfaces through which small as well as the large scale heat transfer is encountered. Distribution of heat transfer along a semi-infinite vertical wavy surface of Newtonian fluid were initially discussed by Yao [9] and Moulic and Yao [10]. Keeping in view ([9]-[10]), several investigations have been done by taking practical situations into account (see Ref. ([11]-[21]) and reported significant effects of surface non-uniformities on fluid flow distribution.

In this study, an attempt has been made to report the influence of surface waviness on natural convection boundary layer flow of the fluid having temperature dependent thermophysical properties. It is assumed that the influence of variable properties of the fluid is confined into the region near the wavy geometry and remains uniform in the main stream. In this study, assumptions have been made that i) the viscosity and thermal conductivity as $\mu \approx T^{n_\mu}$ and $\kappa \approx T^{n_\lambda}$, respectively, ii) the density as inversely proportional to the absolute temperature, and iii) specific heat at constant pressure, c_p, and the Prandtl number, Pr, as

uniform. Taking Grashof number Gr to be very large, the boundary layer approximation is invoked leading to a set of non-similar parabolic partial differential equations whose solution is obtained through implicit finite difference method. The detailed numerical results are displayed in the form of skin friction coefficient, heat transfer rate, velocity and temperature profiles by varying several controlling parameters.

2 Consideration of Variable Thermophysical Properties and Problem Formulation

For the analysis of natural convection, the thermodynamic temperature of the fluid away from the wavy surface of the plate, T_∞, can be taken as the reference temperature. The variable viscosity and thermal conductivity of the fluid is assumed to be temperature dependent and mathematically expressed as:

$$\begin{aligned} \mu/\mu_\infty &= (T/T_\infty)^{n_\mu} \\ \kappa/\kappa_\infty &= (T/T_\infty)^{n_\lambda} \end{aligned} \tag{1}$$

while the variation in density with thermodynamic temperature at uniform pressure are assumed as:

$$\rho/\rho_\infty = (T/T_\infty)^{-1} \tag{2}$$

or

$$\nu/\nu_\infty = (T/T_\infty)^{n_\mu+1} \tag{3}$$

where the values of n_μ and n_λ are taken from the analysis of Hisenrath *et al.* [7], which is based on the summarized experimental values of μ and κ for several monoatomic and diatomic gases, and also for air and water vapours.

In the present analysis, the vertical plate with transverse sinusoidal undulations is situated in viscous incompressible fluid (see Fig. 1). In particular, we assume that the surface profile is given by:

$$y_w = \sigma(x) = a \sin\left(\frac{2\pi x}{L}\right) \tag{4}$$

where a represents the amplitude of the transverse surface wave and L the characteristic length associated with the wave. We have considered the incompressible fluid, which is originally at rest along a vertical wavy plate. Suddenly, the surface of the plate at $y = 0$ is heated with temperature T_w and natural convection starts due to this. The equations describing the complete description of the convective flow along the vertical surface can be written in dimensional form as:

$$\frac{\partial \rho u}{\partial x} + \frac{\partial \rho v}{\partial y} = 0 \tag{5}$$

$$\rho\left(u\frac{\partial u}{\partial x} + v\frac{\partial u}{\partial y}\right) = -\frac{\partial p}{\partial x} + \mu\left(\frac{\partial^2 u}{\partial x^2} + \frac{\partial^2 u}{\partial y^2}\right) + \frac{\partial \mu}{\partial x}\frac{\partial u}{\partial x} + \frac{\partial \mu}{\partial y}\frac{\partial u}{\partial y} + \frac{\rho g\,(T - T_\infty)}{T_\infty} \tag{6}$$

$$\rho\left(u\frac{\partial v}{\partial x} + v\frac{\partial v}{\partial y}\right) = -\frac{\partial p}{\partial y} + \mu\left(\frac{\partial^2 v}{\partial x^2} + \frac{\partial^2 v}{\partial y^2}\right) + \frac{\partial \mu}{\partial x}\frac{\partial v}{\partial x} + \frac{\partial \mu}{\partial y}\frac{\partial v}{\partial y} \tag{7}$$

$$\rho c_p\left(u\frac{\partial T}{\partial x} + v\frac{\partial T}{\partial y}\right) = \frac{\partial}{\partial x}\left(\kappa\frac{\partial T}{\partial x}\right) + \frac{\partial}{\partial y}\left(\kappa\frac{\partial T}{\partial y}\right) \tag{8}$$

where (u, v), T, p, ρ, c_p, κ, g and μ are respectively the velocity vector in the (x, y) direction, temperature, pressure, density, specific heat at constant pressure, thermal conductivity, the gravitational acceleration and dynamic viscosity of the fluid. The fundamental equations stated above are to be solved under appropriate boundary conditions. Therefore, the boundary conditions for the problem under considerations are:

$$\begin{aligned} u(x, y_w) = v(x, y_w) = T(x, y_w) - T_w = 0 \\ u(x, \infty) = T(x, \infty) - T_\infty = 0 \end{aligned} \tag{9}$$

where T_∞ symbolize the ambient fluid temperature such that $T_w >> T_\infty$. To invoke dimensionless equations, following variables are introduced in Eqs. (1)-(9):

$$\begin{aligned} X = \frac{x}{L}, \quad Y = \frac{y - \sigma(x)}{L}Gr^{1/4}, \quad u = \frac{\nu_0}{L}Gr^{1/2}U, \quad v = \frac{\nu_0}{L}Gr^{1/4}\left(V + \sigma_x Gr^{1/4}U\right), \\ P = \frac{L^2}{\rho\nu_0^2 Gr}p, \quad \theta = \frac{T - T_\infty}{T_w - T_\infty}, \lambda = \frac{T_w - T_\infty}{T_\infty}, \quad Gr = \frac{g(T_w - T_\infty)L^3}{\nu^2} \end{aligned} \tag{10}$$

By incorporating Eq. (10), the dimensional continuity, momentum and temperature equa-

tions will be transformed in the underlying form:

$$\frac{\partial U}{\partial X}+\frac{\partial V}{\partial Y}+\frac{1}{\rho}\left(U\frac{\partial \rho}{\partial X}+V\frac{\partial \rho}{\partial Y}\right)=0 \tag{11}$$

$$U\frac{\partial U}{\partial X}+V\frac{\partial U}{\partial Y}=-\frac{\partial P}{\partial X}+\sigma_X Gr^{1/4}\frac{\partial P}{\partial Y}+\frac{\nu}{\nu_0}(1+\sigma_X^2)\left(\frac{\partial^2 U}{\partial Y^2}+\frac{1}{\mu}\frac{\partial \mu}{\partial Y}\frac{\partial U}{\partial Y}\right)+\theta \tag{12}$$

$$\sigma_X\left(U\frac{\partial U}{\partial X}+V\frac{\partial U}{\partial Y}\right)+\sigma_{XX}U^2=-Gr^{1/4}\frac{\partial P}{\partial Y}+\frac{\nu}{\nu_0}\sigma_X(1+\sigma_X^2)\left(\frac{\partial^2 U}{\partial Y^2}+\frac{1}{\mu}\frac{\partial \mu}{\partial Y}\frac{\partial U}{\partial Y}\right) \tag{13}$$

$$\frac{\nu_0}{\nu}\left(U\frac{\partial \theta}{\partial X}+V\frac{\partial \theta}{\partial Y}\right)=\frac{(1+\sigma_X^2)}{\mathrm{Pr}}\left(\frac{\partial^2 \theta}{\partial Y^2}+\frac{1}{\kappa}\frac{\partial \kappa}{\partial Y}\frac{\partial \theta}{\partial Y}\right) \tag{14}$$

where, Gr and Pr are respectively the dimensionless Grashof number and Prandtl number. As it can be noted form Eq. (12) that the pressure gradient is of order $O(Gr^{-1/4})$ along the normal Y direction, which implies that the lower order of pressure gradient along X direction can be determined from the inviscid flow solution. However, due to the fact that there is no externally induced free stream, this pressure gradient is taken as zero, i.e, $\partial P/\partial X=0$. Furthermore, Eq. (12) indicates that the term $Gr^{1/4}\partial P/\partial Y$ is of O (1) and can be determined by the left-hand side of this equation. Thus by eliminating the term $\partial P/\partial Y$ form Eqs. (12) and (13), we will have the following form of momentum equation:

$$\frac{\nu_0}{\nu}\left(U\frac{\partial U}{\partial X}+V\frac{\partial U}{\partial Y}+\frac{\sigma_X\sigma_{XX}}{(1+\sigma_X^2)}U^2-\frac{\theta}{(1+\sigma_X^2)}\right)=(1+\sigma_X^2)\left(\frac{\partial^2 U}{\partial Y^2}+\frac{1}{\mu}\frac{\partial \mu}{\partial Y}\frac{\partial U}{\partial Y}\right) \tag{15}$$

The dimensionless form of the boundary conditions for present analysis is:

$$\begin{gathered}U(X,0)=V(X,0)=\theta(X,0)-1=0\\ U(X,\infty)=\theta(X,\infty)=0\end{gathered} \tag{16}$$

Now, we propose to integrate the above system of equations numerically. Before applying the numerical scheme, these equations are transformed to suitable form with the help of primitive variable formulations. To establish the solutions of the coupled equations (11), (14), and (15) subject to the boundary conditions in (16), we switch into another system

of equations with the help of following set of continuous transformations:

$$X=\xi,\quad Y=X^{\frac{1}{4}}\eta,\quad U(X,Y)=X^{\frac{1}{2}}\overline{U}(\xi,\eta),\quad V(X,Y)=X^{-\frac{1}{4}}\overline{V}(\xi,\eta),\quad \theta(X,Y)=\Theta(\xi,\eta) \tag{17}$$

The above system of equations will be mapped into the following system of parabolic partial differential equations (after dropping bars):

$$\frac{1}{2}U+\xi\frac{\partial U}{\partial\xi}-\frac{1}{4}\eta\frac{\partial U}{\partial\eta}+\frac{\partial V}{\partial\eta}+\frac{1}{\rho}\left(\xi U\frac{\partial\rho}{\partial\xi}+\left(V-\frac{1}{4}\eta U\right)\frac{\partial\rho}{\partial\eta}\right)=0 \tag{18}$$

$$\frac{\nu_0}{\nu}\left[\left(\frac{1}{2}+\frac{\xi\sigma_\xi\sigma_{\xi\xi}}{(1+\sigma_\xi^2)}\right)U^2+\xi U\frac{\partial U}{\partial\xi}+\left(V-\frac{1}{4}\eta U\right)\frac{\partial U}{\partial\eta}-\frac{\Theta}{(1+\sigma_\xi^2)}\right]=(1+\sigma_\xi^2)\left(\frac{\partial^2U}{\partial Y^2}+\frac{1}{\mu}\frac{\partial\mu}{\partial\eta}\frac{\partial U}{\partial\eta}\right) \tag{19}$$

$$\frac{\nu_0}{\nu}\left[\xi U\frac{\partial\Theta}{\partial\xi}+\left(V-\frac{1}{4}\eta U\right)\frac{\partial\Theta}{\partial\eta}\right]=\frac{(1+\sigma_\xi^2)}{\Pr}\left(\frac{\partial^2\Theta}{\partial Y^2}+\frac{1}{\kappa}\frac{\partial\kappa}{\partial\eta}\frac{\partial\Theta}{\partial\eta}\right) \tag{20}$$

From equations (1)-(4) combined with equations (10) and (17), we have:

$$\frac{1}{\rho}\frac{\partial\rho}{\partial\eta}=-\frac{\lambda}{(1+\lambda\Theta)}\frac{\partial\Theta}{\partial\eta},\quad \frac{1}{\rho}\frac{\partial\rho}{\partial\xi}=-\frac{\lambda}{(1+\lambda\Theta)}\frac{\partial\Theta}{\partial\xi} \tag{21}$$

$$\frac{1}{\rho}\frac{\partial\mu}{\partial\eta}=\frac{\lambda n_\mu}{(1+\lambda\Theta)}\frac{\partial\Theta}{\partial\eta},\quad \frac{1}{\rho}\frac{\partial\kappa}{\partial\eta}=\frac{\lambda n_\lambda}{(1+\lambda\Theta)}\frac{\partial\Theta}{\partial\eta} \tag{22}$$

and

$$\frac{\nu_0}{\nu}=(1+\lambda\Theta)^{-(1+n_\mu)} \tag{23}$$

where, $\lambda=(T_w-T_\infty)/T_\infty$. Now by incorporating the equations form (21)-(23) in the system of equations (18)-(20), we will have:

$$\frac{1}{2}U+\xi\frac{\partial U}{\partial\xi}-\frac{1}{4}\eta\frac{\partial U}{\partial\eta}+\frac{\partial V}{\partial\eta}-\frac{\lambda}{(1+\lambda\Theta)}\left(\xi U\frac{\partial\Theta}{\partial\xi}+\left(V-\frac{1}{4}\eta U\right)\frac{\partial\Theta}{\partial\eta}\right)=0 \tag{24}$$

$$(1+\lambda\Theta)^{-(1+n_\mu)}\left[\left(\frac{1}{2}+\frac{\xi\sigma_\xi\sigma_{\xi\xi}}{(1+\sigma_\xi^2)}\right)U^2+\xi U\frac{\partial U}{\partial\xi}+\left(V-\frac{1}{4}\eta U\right)\frac{\partial U}{\partial\eta}-\frac{\Theta}{(1+\sigma_\xi^2)}\right]=(1+\sigma_\xi^2)\left(\frac{\partial^2U}{\partial\eta^2}+\frac{\lambda n_\mu}{(1+\lambda\Theta)}\frac{\partial\Theta}{\partial\eta}\frac{\partial U}{\partial\eta}\right) \tag{25}$$

$$(1+\lambda\Theta)^{-(1+n_\mu)}\left[\xi U\frac{\partial\Theta}{\partial\xi}+\left(V-\frac{1}{4}\eta U\right)\frac{\partial\Theta}{\partial\eta}\right]=\frac{(1+\sigma_\xi^2)}{\mathrm{Pr}}\left(\frac{\partial^2\Theta}{\partial\eta^2}+\frac{\lambda n_\lambda}{(1+\lambda\Theta)}\left(\frac{\partial\Theta}{\partial\eta}\right)^2\right) \tag{26}$$

subject to the boundary conditions:

$$\begin{gathered} U(\xi,0)=V(\xi,0)=\Theta(\xi,0)-1=0 \\ U(\xi,\infty)=\Theta(\xi,0)=0 \end{gathered} \tag{27}$$

A numerical solution for the coupled system of non linear partial differential Eqs. (24)-(27) by a finite difference method is straightforward, since the computational grids can be fitted to the body shape in (ξ,η) coordinates. The discretization process is carried out by exploiting the central difference quotients for diffusion terms, and the forward difference for the convection terms. The computational process is started at $\xi = 0.0$ as the singularity at this point has been removed by the scaling. At every ξ station, the computations are iterated until the difference of the results, of two successive iterations become less or equal to 10^{-6}. In order to get accurate results, we have compared the results at different grid size in η direction and reached at the conclusion to chose $\Delta\eta = 0.003$. In this integration, the maximum value of η is taken to be 50.0. A detail description of discretization procedure and numerical scheme is presented in [22].

Once the unknown variables of both phases are obtained, the measurable physical quantities like local skin friction coefficient, τ_w, and rate of heat transfer, Q_w, are used to express the solutions of the current scenario. These quantities are much significant from engineering point of view, as both can be served to improve specifically the efficiency and shape of many equipments in aerodynamics. The metamathematical expressions for these physical quantities takes the underlying form:

$$\begin{aligned} \tau_w &= C_f\left(\frac{Gr^{-3}}{\xi}\right)^{1/4}=(1+\lambda)^{-(n_\mu+1)}\sqrt{1+\sigma_\xi^2}\left(\frac{\partial U}{\partial\eta}\right)_{\eta=0} \\ Q_w &= Nu\left(\frac{Gr}{\xi}\right)^{-1/4}=-(1+\lambda)^{n_\lambda}\sqrt{1+\sigma_\xi^2}\left(\frac{\partial\Theta}{\partial\eta}\right)_{\eta=0} \end{aligned} \tag{28}$$

In case of uniform thermophysical properties, these expressions takes the underlying for:

$$\begin{aligned} \tau_w &= C_f \left(\frac{Gr^{-3}}{\xi}\right)^{1/4} = \sqrt{1+\sigma_\xi^2}\left(\frac{\partial U}{\partial \eta}\right)_{\eta=0} \\ Q_w &= Nu \left(\frac{Gr}{\xi}\right)^{-1/4} = -\sqrt{1+\sigma_\xi^2}\left(\frac{\partial \Theta}{\partial \eta}\right)_{\eta=0} \end{aligned} \tag{29}$$

Now the numerical results obtained for the key parameters are discussed in the section below.

3 Numerical Results and Discussion

The prime interest of the present study is to report the influence of variable thermophysical properties parameters, n_μ, n_λ and λ on heat transfer and skin friction coefficient, velocity and temperature profiles. We performed two-dimensional simulations in order to obtain solutions of mathematical model presented in terms of primitive variables given in Eqs. (24-27) from the two-point implicit finite difference method. Numerical results are reported for the overall effectiveness of variable thermophycial properties of gases moving along a transverse geometry. As the influence of temperature dependent properties is more pronounced for gases, therefore, present numerical solutions are performed by taking air (i.e., $(\mathrm{Pr} = 0.7, n_\mu = 0.68, n_\lambda = 0.81)$ as a participating fluid. The parametric values for air and other gases are taken from study of Shang and Wang ([8]), while the values of other parameters are taken as: $\lambda = (0.0, 1.0, 2.0)$ and $a = (0.0, 0.1, 0.3)$.

In order to ensure the accuracy of our scheme and computational data, comparison is also being made with already available published data. It should be noted that the numerical results obtained herein, reduce to those reported by Shang and Wang ([8]) provided the amplitude of wavy surface parameter is taken as zero. The results are compared in tabular form and computational data is entered in Table 1 and 2 which shows quite an excellent agreement between the two studies. Here, the calculated results for different gases agree well with those reported in [8] (see Table 1 and 2). Besides, it is important to mention here that, values of rate of heat transfer rates, both at the surface and in free stream region, i.e, $Nu_{(x,w)}/(Gr_{(x,w)})^{1/4}$ and $Nu_{(x,\infty)}/(Gr_{(x,\infty)})^{1/4}$, for various gases at different values of

λ are compared and summarized in Table 2. Furthermore, the present model recovers the solutions reported by Yao [9] provided that the thermophysical properties of the gas are taken as uniform. In [9], Keller box method is used to obtain solutions over the whole range of axial coordinate ξ, while the present computational results are obtained from implicit finite difference method. In-spite of different formulations and methods as well, the computational results for Nusslet number coefficient are compared in Fig. 2 by keeping the physical parameters as: $\Pr = 1.0$, $a = (0.1, 0.3)$ and $(\lambda = n_\mu = n_\lambda = 0.0)$. The graphical data shows quite an excellent agreement between the two studies and this comparison also validates our numerical scheme.

Table 1: The comparison between calculated values of $-(\partial\Theta/\partial\eta)_{\eta=0}$ and those reported in Ref. [8].

T_w/T_∞	Ar $\Pr = 0.622$ $n_\mu = 0.72$ $n_\lambda = 0.73$		H_2 $\Pr = 0.68$ $n_\mu = 0.68$ $n_\lambda = 0.8$		Air $\Pr = 0.7$ $n_\mu = 0.68$ $n_\lambda = 0.81$		N_2 $\Pr = 0.71$ $n_\mu = 0.67$ $n_\lambda = 0.76$	
	Ref. [8]	Present	Ref. [8]	Present	Ref. [8]	Present	Ref. [8]	Present
3	0.1940	0.19388	0.1974	0.19736	0.1987	0.19868	0.2043	0.20432
5/2	0.2256	0.22559	0.2300	0.22995	0.2316	0.23160	0.2374	0.23742
2	0.2714	0.27133	0.2772	0.27719	0.2794	0.27938	0.2852	0.28518
3/2	0.3438	0.34375	0.3526	0.35254	0.3557	0.35568	0.3609	0.36091
5/4	0.3990	0.39902	0.4105	0.41045	0.4188	0.41878	0.4172	0.41715
3/4	0.6035	0.60358	0.6276	0.62769	0.6351	0.63518	0.6336	0.63374
1/2	0.8334	0.83483	0.8774	0.87793	0.8898	0.89027	0.8776	0.87810

In order to show the geometric influence of variation of amplitude of wavy surface parameter, a, on τ_w and Q_w, Fig. 3 is plotted. For comparison, the behavior of physical quantities along flat vertical plate (i.e, $a = 0.0$) is also presented. It is evident from the figures that both the skin friction coefficient and the rate of heat transfer are uniform all over the plate, if the amplitude of the vertical plate is zero. The change in surface contour is followed by raise and fall of the curves. As it can be visualize from Fig. 3, that the effect of amplitude of the vertical surface a, on average, is to minimize both physical quantities. But it is interesting to see that the large values of a are a major factor to increase the amplitude of the sinusoidal waves and the maximum values of skin friction and rate of heat transfer occur on the crests of the wavy surface while the minimum values occur on the

Table 2: The comparison between calculated values of $Nu_{(x,\infty)}/(Gr_{(x,\infty)})^{1/4}$ and $Nu_{(x,w)}/(Gr_{(x,w)})^{1/4}$ with those reported in Ref. [8].

T_w/T_∞	Ar Pr = 0.622 $n_\mu = 0.72$ $n_\lambda = 0.73$		H_2 Pr = 0.68 $n_\mu = 0.68$ $n_\lambda = 0.8$		Air Pr = 0.7 $n_\mu = 0.68$ $n_\lambda = 0.81$		N_2 Pr = 0.71 $n_\mu = 0.67$ $n_\lambda = 0.76$	
	$Nu_{(x,\infty)}/(Gr_{(x,\infty)})^{1/4}$							
	Ref. [8]	Present	Ref. [8]	Present	Ref. [8]	Present	Ref. [8]	Present
3	0.306	0.30572	0.336	0.33607	0.342	0.34206	0.333	0.33298
5/2	0.311	0.31139	0.338	0.33843	0.344	0.34400	0.337	0.33685
2	0.319	0.31823	0.341	0.34126	0.347	0.34635	0.341	0.34150
3/2	0.326	0.32680	0.345	0.34480	0.350	0.34929	0.347	0.34730
1	0.339	0.33830	0.350	0.34951	0.354	0.35321	0.356	0.35503
	$Nu_{(x,w)}/(Gr_{(x,w)})^{1/4}$							
3	0.353	0.35265	0.351	0.35117	0.354	0.35352	0.362	0.36157
5/2	0.350	0.35079	0.351	0.35106	0.354	0.35359	0.361	0.36081
2	0.347	0.34823	0.351	0.35085	0.354	0.35363	0.360	0.35972
3/2	0.344	0.34449	0.350	0.35043	0.354	0.35356	0.358	0.35803
1	0.339	0.33830	0.350	0.34951	0.354	0.35321	0.356	0.35503

troughs. Particularly, the rate of heat transfer is significantly affected by increasing the fluctuations in sinusoidal waves. As it can be seen from Fig. 3(b) that the rate of heat transfer is maximum for flat surface ($a = 0.0$). This may happen because the thermal resistance increases as the fluid accumulates between the trough and crest, and ultimately the rate of heat transfer is reduced near the leading edge.

Influence of parameter, λ on skin friction coefficient, τ_w and local rate of heat transfer coefficient Q_w is also presented graphically in Fig. 4. Here, the parameter λ varies between 0 and 2, and it should be noted that $\lambda \simeq 0.0$ corresponds to the case for small temperature difference between the surface and the fluid ($T_w - T_\infty \simeq 0$) and indicating that buoyancy approximation becomes valid. However, for high temperature difference variable thermophysical properties of air are considered which depicts considerable variation in the numerical values of local skin friction and rate of heat transfer. As it can be inferred from Fig. 4, that both the skin friction coefficient and rate of heat transfer undergoes a considerable decline by increasing the parameter λ. Particularly, the amplitude of the waves representing the skin friction coefficient in Fig. 4(a) is sufficiently become small for non-zero values of λ. This may happen because, the air with variable density and viscosity becomes

less dense and viscous due to large temperature variations, which ultimately reduces the frictional forces near the vicinity of wavy plate. Similar behavior is observed in Fig. 4(b), the heat transfer rate is very low across the wavy surface for high λ which indicates that λ acts as a retarding force for Q_w. Such behavior is quite usual because the variable thermophysical properties of air significantly affect the heat transport phenomenon. It is important to mention here that, $\lambda = 0.0$ recovers the solutions for free convection of viscous fluid model with uniform properties.

In order to make the comparison of skin friction coefficients and rate of heat transfer of different gases, Fig. 5 is plotted. For this, numerical computations are made for some practical examples, such that, i) air ($\mathrm{Pr} = 0.7, n_\mu = 0.68, n_\lambda = 0.81$), ii) O_2($\mathrm{Pr} = 0.733, n_\mu = 0.694, n_\lambda = 0.86$) and iii) water vapour ($\mathrm{Pr} = 1.0, n_\mu = 1.04, n_\lambda = 1.185$) and these values are taken from the study of Shang and Wang [8]. It is observed from Fig. 5(a), that the skin friction coefficient is same for air and O_2, but not in case of water vapour. The physical reason for this behavior may be apprehended to the fact that the air contains a very small amount of water vapour, i.e, on average around 1% at sea level, and 0.4% over the entire atmosphere. Sice, the ratio of water vapour in air is too low as compared to other gases, therefore, the behavior of τ_w is not the same as that of O_2 and many other gases in air. More interestingly, the rate of heat transfer is maximum when the water vapoour are penetrated into the mechanism (see Fig. 5(b)). Since the air is composition of all raw gases, therefore, Q_w is too low for the case of air, whereas, its shows its maximum value for water vapour. It is important to mention here that, not only the magnitude of Q_w increases for water vapours but also the amplitude of the pure sinusoidal waveform get intensified. The entire convective regime is hotter for the case of water vapour and the large temperature gradient in the thermal boundary layer promotes conductive heating near the surface of the plate.

In order to determine the influence of variable thermophysical properties of gases on skin frcition coefficient and rate of heat transfer, Fig. 6 is plotted. For comparative analysis, τ_w and Q_w for air and water vapour having uniform properties are also presented. As it can be seen from Fig. 6(a), that the skin friction is higher for the air with constant properties and it shows reduction when the physical properties of air are taken as temper-

ature dependent. As mentioned earlier, air get less dense and less viscous with respect to variation in temperature, and ultimately, the frictional forces becomes less influential in the boundary layer region. Similar behavior is recorded for the case of water vapour (see Fig. 6(a)). Furthermore, it is observed from the Fig. 6(b) that variable properties has notable effect on heat transfer rate. More interestingly, the rate of heat transfer is more likely to be intensified for the case of water vapour as compared to the air.

Fig. 7 is plotted to visualize the detailed scenario of velocity and temperature profile for various values of amplitude of wavy surface a. As it can clearly seen form Fig. 7(a), that the velocity of the air decreases significantly owing to increase in value of amplitude a. Such behavior is expected, because when amplitude of the wavy surface increases, the air between crust and trough of the waves undergoes more resistance to flow and hence fluid velocity decreases. As, small values of a offers no resistance to flow and gas quickly attains its asymptotic value in the boundary layer region. However, the parameter a has reverse affect on temperature profile (see Fig. 7(b)). This may happens due to the fact that, the air particles near the surface attains the thermal energy from the hotter surface of large amplitude and ultimately give rise to the temperature of air in whole convective regime. Thus, the large values of surface amplitude acts as a delaying factor for gas velocity as well as temperature profiles to reach their limiting value.

Fig. 8 anticipates the influence of parameter λ on velocity and temperature profiles. It is inferred from Fig. 8 that parameter λ has notable influence on velocity as well as on temperature profiles of air. The plots in Fig. 8 reveals the fact that non-zero values of λ participates in magnifying the velocity and temperature profile. Particularly, non-zero values of λ acts like a supportive driving force that accelerates the temperature of the air within the boundary layer region.

The effect of parameters variable thermophysical properties on velocity and temperature profiles of air and water vapour is illustrated in Fig. 9. For comparison, velocity and temperature profiles for air and water vapour with uniform properties are also presented. It is noteworthy to mention here that, $(n_\mu = n_\lambda = 0.0)$ corresponds to the case all the properties of the air and water vapour are taken as uniform. The curve in Fig. 9 show that, velocity and temperature profiles for both air and water vapour shows a considerable

incline for non-zero values of parameters n_μ and n_λ. For the case of uniform thermophysical properties, the velocity as well as temperature profiles decays quickly to their asymptotical values and approaches to zero in the free stream region.

4 Conclusion

This paper aims to compute the effects of variable thermophysical properties on natural convection flow along a vertical wavy heated plate. The nonlinear system of boundary layer equations are iteratively solved step-by-step by using implicit finite difference method along with tri-diagonal solver. The problem is investigated to predict the characteristics of free convection for the gases having non-uniform properties moving along a transverse geometry. Computational results are shown for the physical quantities, namely, skin friction coefficient, rate of heat transfer, velocity and temperature profiles. The solutions are established for a range of physically important parameters which emerge from the variable thermophysical properties of the gas together with the sinusoidal wave form geometry. It is concluded that the heat transfer coefficient near the surface of the wavy plate is considerably reduced for the air with variable properties.

References

[1] Sparrow, E. M., Gregg, J. L., The variable fluid property problem in free convection, *Trans. ASME*, **80**, 1958, 879-886.

[2] Brown, A., The effect on laminar free convection heat transfer of temperature dependence of the coefficient of volumetric expansion, *J. Heat Transfer*, **97**, 1975, 133-135.

[3] Gray, D. D., Giogini, A., The validity of the Boussinesq approximation for liquids and gases, *Int. J. Heat Mass Transfer*, **19**, 1977, 545-551.

[4] Clausing, A. M., Kempka, S. N., The influences of property variations on natural convection from vertical surfaces, *J. Heat Transfer*, **103**, 1981, 609-612.

[5] Gebhart, B., Natural convection flow, instability, and transition, *J. Heat Transfer*, **91**, 1969, 293-309.

[6] Eckert, E. R. G., Drake, R. M., Analysis of Hear and Mass Transfer. McGraw-Hill, New York, 1972.

[7] Hisenrath, J., Tables of thermodynamic and transport properties, *National Bureau of Standards*, 1955.

[8] Shang, D. Y., Wang, B. X., Effect of variable thermophysical properties on laminar free convection of gas, *Int. J. Heat Mass Transfer*, **33**, 1990, 1387-1395.

[9] Yao, L. S., Natural convection along a vertical wavy surface, *J. Heat Transfer*, **105**, 1983, 465-468.

[10] Moulic, S. G., Yao, L. S., Natural convection along a wavy surface with uniform heat flux, *J. Heat Transfer*, **111**, 1989, 1106-1108.

[11] Rees, D. A. S., Pop, I., Free convection induced by a vertical wavy surface with uniform heat flux in a porous medium, *J. Heat Transfer*, **117**, 1995, 545-550.

[12] Hossain, M. A., Pop, I., Magnetohydrodynamic boundary layer flow and heat transfer on a continuous moving wavy surface, *Arch. Mechanics*, **48**, 1996, 813-823.

[13] Hossain, M. A., Rees, D. A. S., Combined heat and mass transfer in natural convection flow from a vertical wavy surface, *Acta Mechanica*, **136**, 1999, 133-141.

[14] Siddiqa, S., Hossain, M. A., Saha, S. C., Natural convection flow with surface radiation along a vertical wavy surface, *Numerical Heat Transfer, Part A: Applications*, **64**, 2013, 400-415.

[15] Siddiqa, S., Hossain, M. A., Saha, S. C., The effect of thermal radiation on the natural convection boundary layer flow over a wavy horizontal surface, *Int. J. of Thermal Sciences*, **84**, 2104, 143-150.

[16] Pop, I., Natural convection of a darcian fluid about a wavy cone, *Int. Commun. Heat Mass transfer*, **21**, 1994, 891-899.

[17] Pop, I., Na, T. Y., Natural convection from a wavy cone, *Appl. Sci. Res.*, **54**, 1995, 125-136.

[18] Pop, I., Na, T. Y., Natural convection over a vertical wavy frustum of a cone, *J. Nonlinear Mechanics*, **34**, 1999, 925-934.

[19] Molla, M. M., Hossain, M. A., Gorla, R. S. R., Radiation effects on natural convection boundary layer flow over a vertical wavy frustum of a cone, *Proc. IMechE Part C: J. Mechanical Engineering Science*, **223**, 2009 1605-1614.

[20] Siddiqa, S., Hina, G., Begum, N., Saleem, S., Hossain, M. A., Gorla, R. S. R., Numerical and analytical solution of nanofluid bioconvection due to gyrotactic microorganisms along a vertical wavy cone, *Int. J. Heat Mass Transfer*, **101**, 2016, 608-613.

[21] Siddiqa, S., Begum, N., Hossain, M. A., Massarotti, N., Influence of thermal radiation on contaminated air and water flow past a vertical wavy frustum of a cone, *Int. Commun. Heat Mass*, **76**, 2016, 63-68.

[22] Siddiqa, S., Begum, N., Hossain, M. A., Radiation effects from an isothermal vertical wavy cone with variable fluid properties, *Appl. Math. Comput.*, **289**, 2016, 149-158.

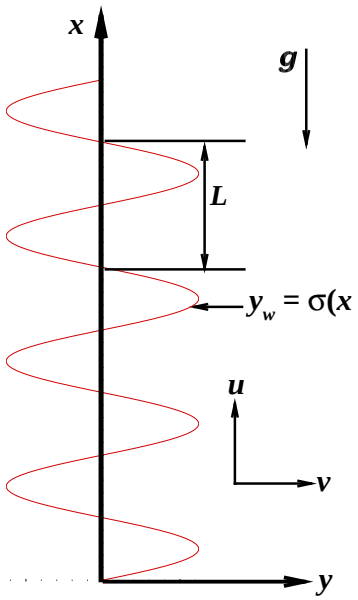

Fig. 1 Schematic of the problem.

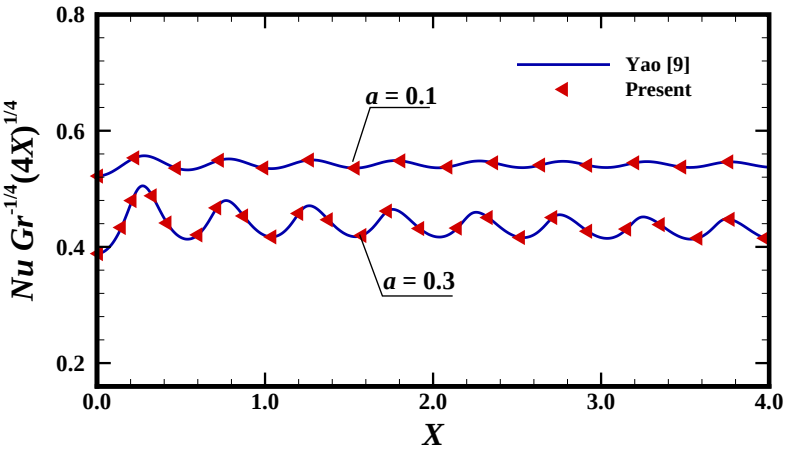

Fig. 2 Local Nusselt number coefficient for $a = 0.1, 0.3$, while Pr $= 1.0$ and $\lambda = n_\mu = n_\lambda = 0.0$.

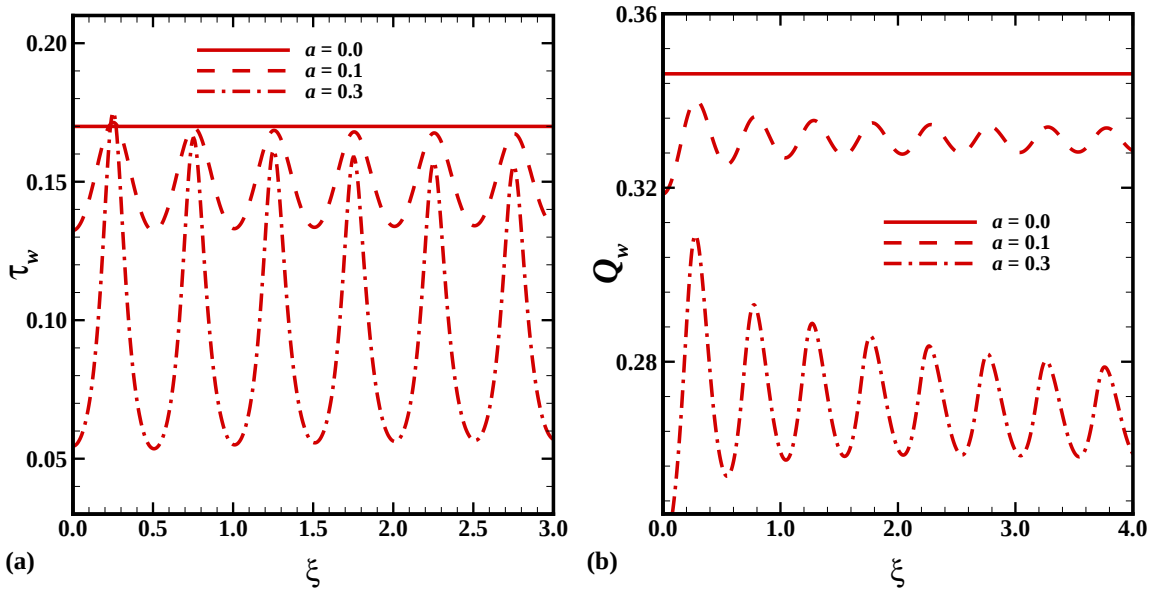

Fig. 3(a) Skin friction and (b) Rate of heat transfer coefficients for $a = (0.0, 0.1, 0.3)$ while Pr $= 0.7$, $n_\lambda = 0.81$, $n_\mu = 0.68$ and $\lambda = 1.0$.

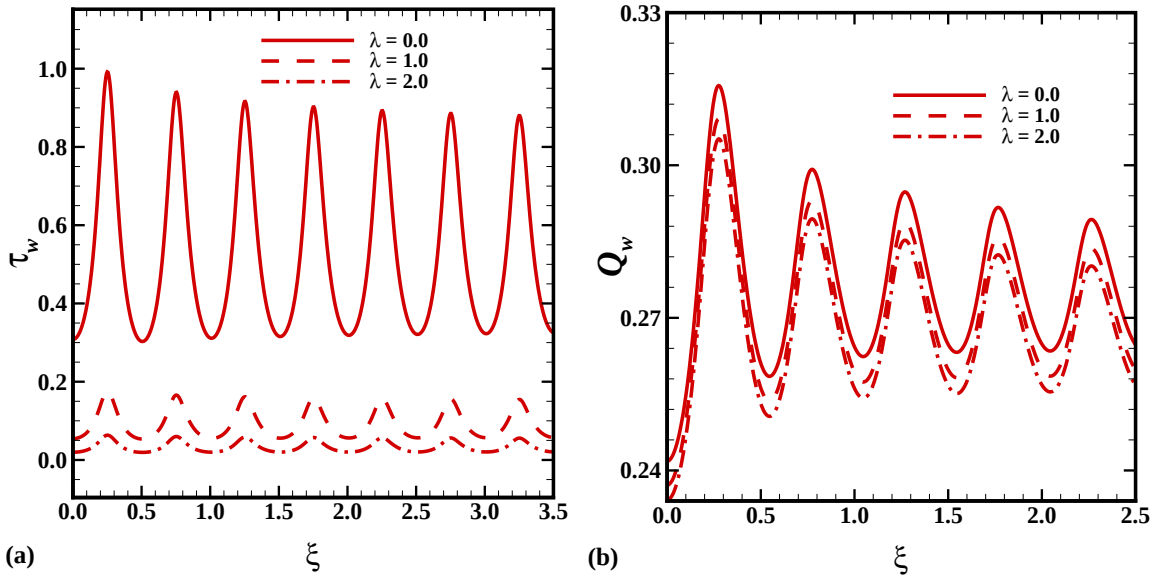

Fig. 4(a) Skin friction and (b) Rate of heat transfer coefficients for $\lambda = (0.0, 1.0, 2.0)$, while Pr $= 0.7$, $a = 0.3$, $n_\lambda = 0.81$ and $n_\mu = 0.68$.

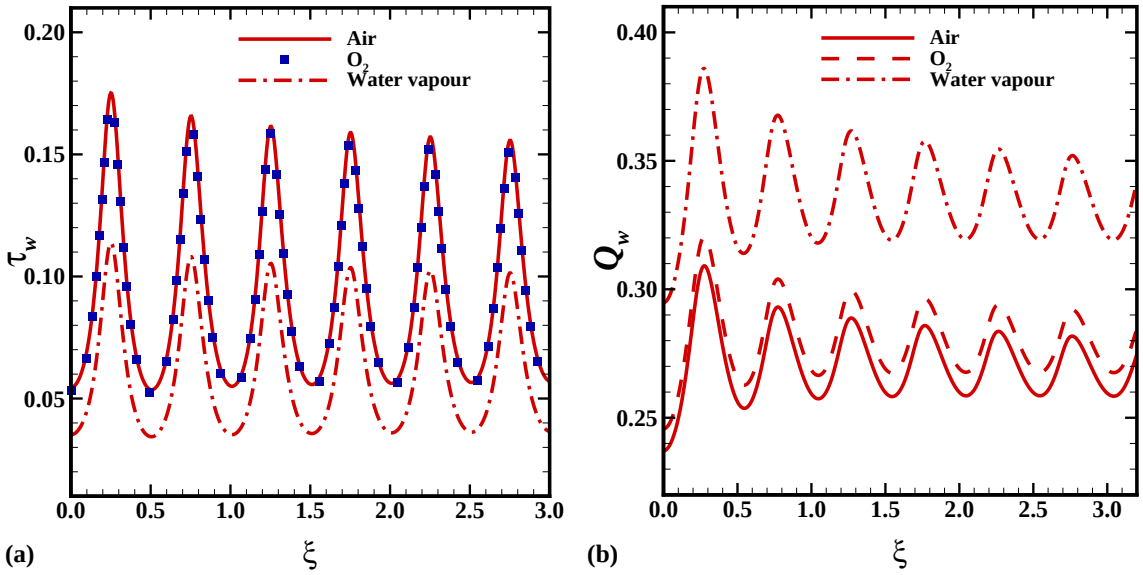

Fig. 5 Comparison of (a) Skin friction coefficients and (b) Rates of heat transfer of Air ($\mathbf{Pr} = 0.7, n_\mu = 0.68, n_\lambda = 0.81$), $\mathbf{O_2}$($\mathbf{Pr} = 0.733, n_\mu = 0.694, n_\lambda = 0.86$) and Water vapour ($\mathbf{Pr} = 1.0, n_\mu = 1.04, n_\lambda = 1.185$) while $a = 0.3$ and $\lambda = 1.0$.

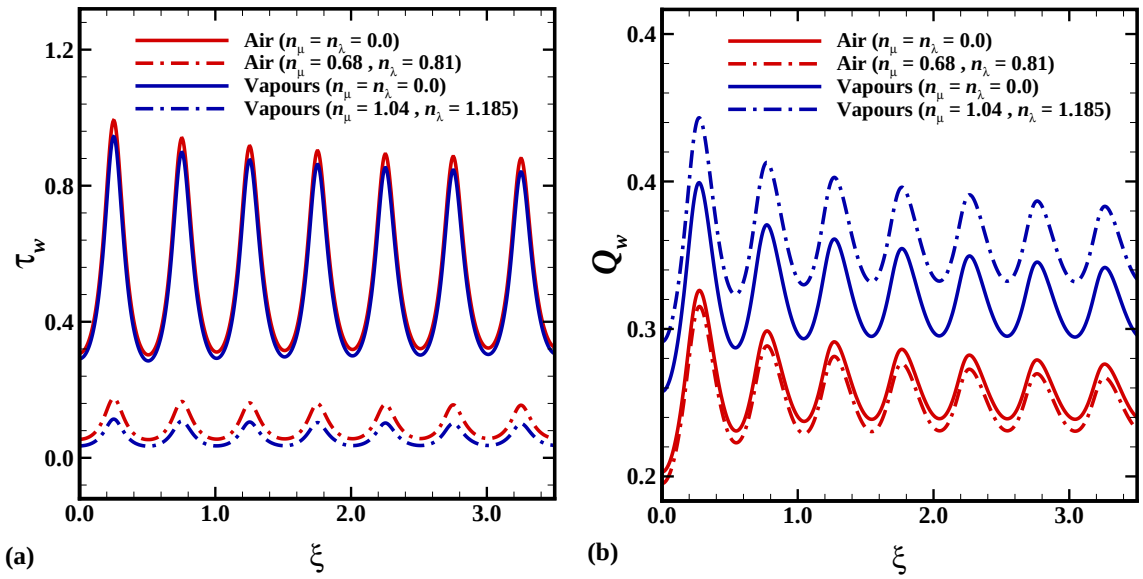

Fig. 6(a) Skin friction and (b) Rate of heat transfer coefficients of Air $(\mathbf{Pr} = 0.7, n_\mu = (0.0, 0.68), n_\lambda = (0.0, 0.81))$ **and Water vapour** $(\mathbf{Pr} = 1.0, n_\mu = (0.0, 1.04), n_\lambda = (0.0, 1.185))$ **while** $a = 0.3$ **and** $\lambda = 1.0$**.**

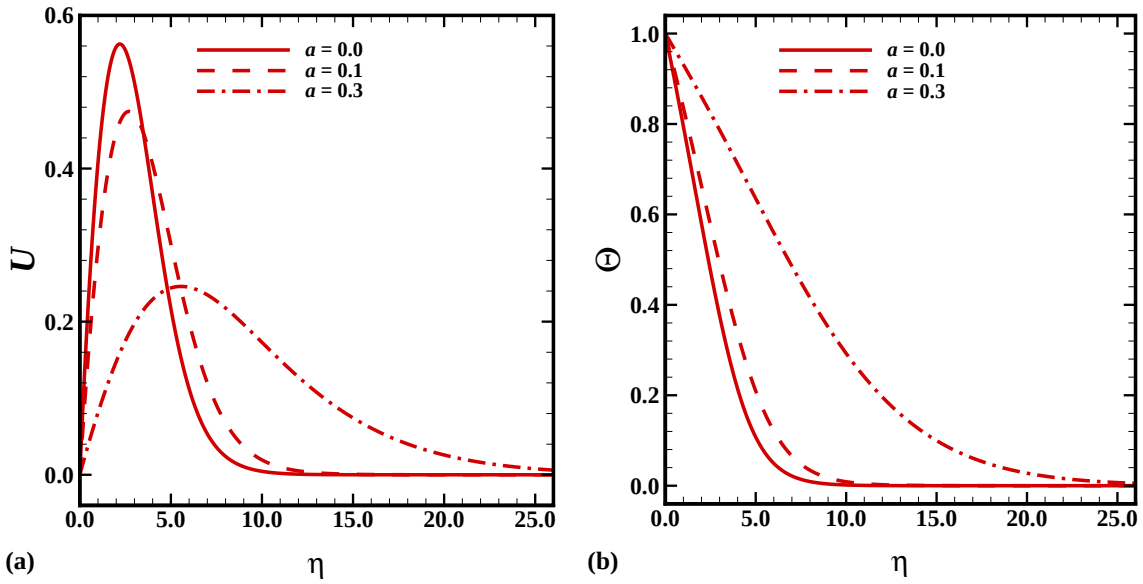

Fig. 7(a) Velocity and (b) Temperature profiles for for $a = (0.0, 0.1, 0.3)$ **while** $\mathbf{Pr} = 0.7$**,** $n_\lambda = 0.81$**,** $n_\mu = 0.68$**,** $\lambda = 1.0$ **and** $\xi = 10.0$**.**

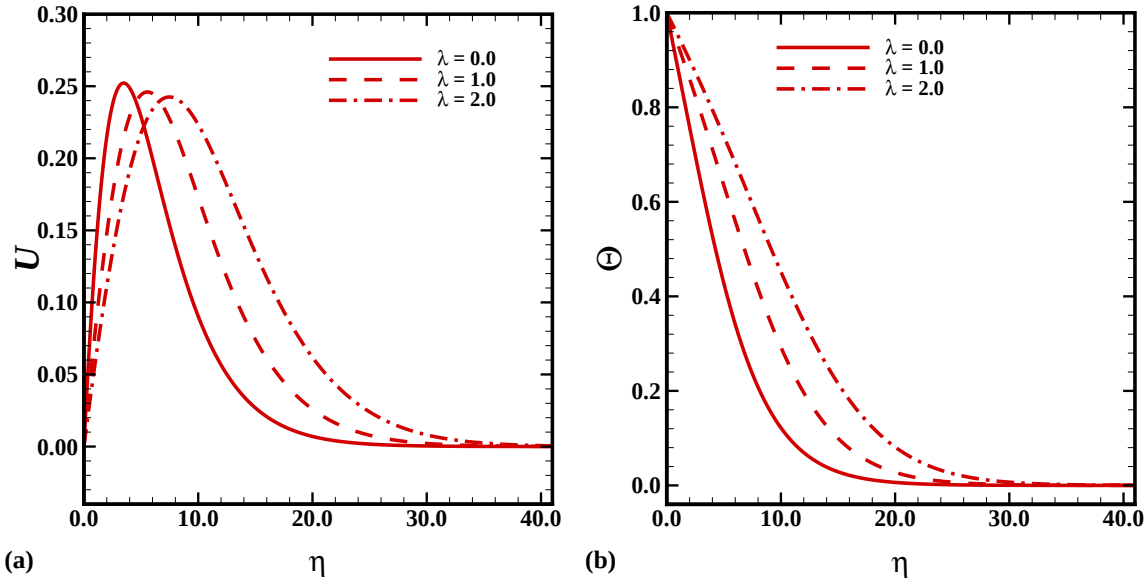

Fig. 8(a) Velocity and (b) Temperature profiles for $\lambda = (0.0, 1.0, 2.0)$, while $\mathbf{Pr} = 0.7$, $a = 0.3$, $n_\lambda = 0.81$, $n_\mu = 0.68$ and $\xi = 10.0$.

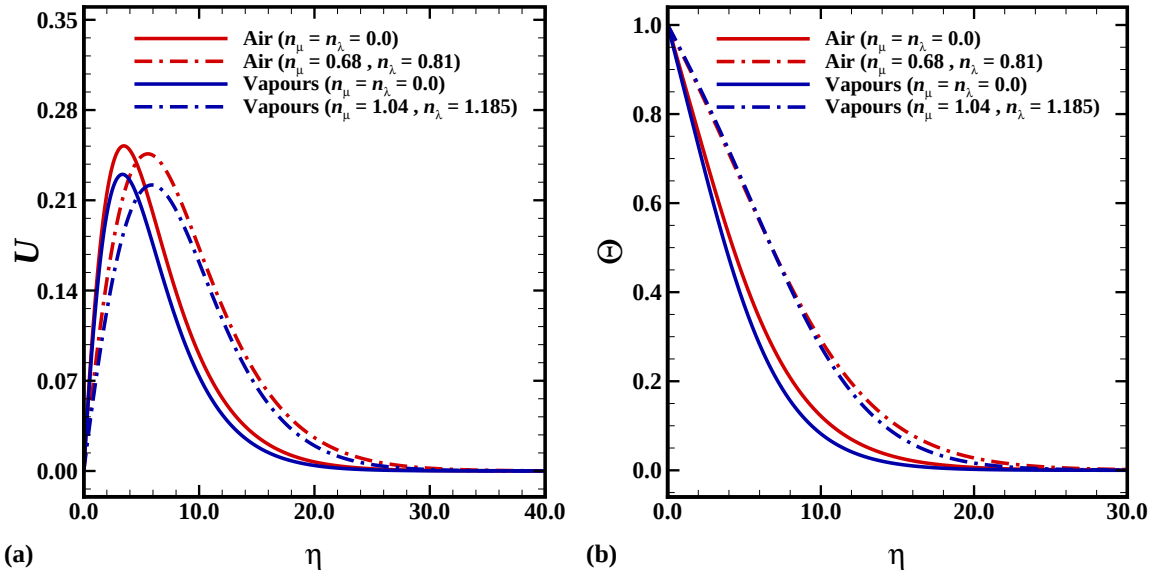

Fig. 9(a) Velocity and (b) Temperature profiles of Air $(\mathbf{Pr} = 0.7, n_\mu = (0.0, 0.68), n_\lambda = (0.0, 0.81))$ and Water vapour $(\mathbf{Pr} = 1.0, n_\mu = (0.0, 1.04), n_\lambda = (0.0, 1.185))$ while $a = 0.3$, $\lambda = 1.0$ and $\xi = 10.0$.